Widespread seismicity excitation throughout central Japan following the 2011 M=9.0 Tohoku earthquake and its interpretation by Coulomb stress transfer

Shinji Toda,[1] Ross S. Stein,[2] and Jian Lin[3]

Received 24 April 2011; revised 22 June 2011; accepted 28 June 2011; published 6 August 2011.

[1] We report on a broad and unprecedented increase in seismicity rate following the M=9.0 Tohoku mainshock for M ≥ 2 earthquakes over inland Japan, parts of the Japan Sea and Izu islands, at distances of up to 425 km from the locus of high (≥15 m) seismic slip on the megathrust. Such an increase was not seen for the 2004 M=9.1 Sumatra or 2010 M=8.8 Chile earthquakes, but they lacked the seismic networks necessary to detect such small events. Here we explore the possibility that the rate changes are the product of static Coulomb stress transfer to small faults. We use the nodal planes of M ≥ 3.5 earthquakes as proxies for such small active faults, and find that of fifteen regions averaging ~80 by 80 km in size, 11 show a positive association between calculated stress changes and the observed seismicity rate change, 3 show a negative correlation, and for one the changes are too small to assess. This work demonstrates that seismicity can turn on in the nominal stress shadow of a mainshock as long as small geometrically diverse active faults exist there, which is likely quite common. **Citation:** Toda, S., R. S. Stein, and J. Lin (2011), Widespread seismicity excitation throughout central Japan following the 2011 M=9.0 Tohoku earthquake and its interpretation by Coulomb stress transfer, *Geophys. Res. Lett.*, *38*, L00G03, doi:10.1029/2011GL047834.

1. Introduction

[2] The M=9.0 Tohoku-chiho Taiheiyo-oki (hereafter, 'Tohoku') earthquake resulted from slip on a roughly 500-km-long and 200-km-wide seismic megathrust source (http://tectonics.caltech.edu/slip_history/2011_taiheiyo-oki/index.html). Many offshore aftershocks, including four M ≥ 7 and ~70 M ≥ 6 shocks, have struck during the ensuing three months. The possibility of other large earthquakes on adjacent portions of the megathrust, similar to the 28 March 2005 M=8.6 Simeulue-Nias earthquake following the 26 December 2004 M=9.1 Sumatra-Andaman earthquake [*Nalbant et al.*, 2005; *Pollitz et al.*, 2006] are thus possible. Sites of potential tsunamigenic earthquakes include the Sanriku-Hokubu area to the north, and Off-Boso (east of the Boso peninsula) to the south [*Headquarters for Earthquake Research Promotion*, 2005] of the 2011 Tohoku rupture.

[3] Equally important for the exposed population and infrastructure would be the occurrence of large inland shocks in northern Honshu. Three M ~ 6 shallow inland earthquakes have struck as far as ~300 km from the M=9 source since the Tohoku mainshock, reaffirming the broad reach and triggering potential of the great quake (Figure 1a). The 11 April 2011 Mj=7.0 (M=6.6) Iwaki earthquake produced 30 km of normal faulting, with a peak surface slip of 2 m. Among such inland sites, none is more important than Tokyo, which was last struck by the 1923 Kanto M=7.9 Sagami megathrust event [*Nyst et al.*, 2006], and a deeper inland event in the 1855 M ~ 7.2 Ansei-Edo earthquake [*Grunewald and Stein*, 2006]. This concern is heightened by several inland large earthquakes in Tohoku that have followed M=7–8 interplate events by months to a decade [*Shimazaki*, 1978; *Seno*, 1979; *Churei*, 2002], including the 31 August 1896 Mj = 7.2 Rikuu earthquake, which produced a 30-km-long surface rupture that devastated the eastern Akita Prefecture, with 200 deaths (Figure 2a).

[4] To evaluate the potential triggering impact of the Tohoku earthquake to inland Japan, we analyze the seismicity rate change since the Tohoku mainshock, and calculate the associated static Coulomb stress changes over the region of seismicity rate change.

2. Inland Seismicity Rate Changes Associated With the Tohoku Earthquake

[5] The widespread seismicity rate increase across central Japan and extending west to the Japan Sea and south to the Izu islands is evident in Figure 1. Broadly, there are strong increases in seismicity rate across a region extending up to 300 km from the distal edges of the M=9 rupture surface, and 425 km from the locus of high (≥15 m) seismic slip. In addition to the microseismicity, an Mj=6.7 earthquake occurred 13 hours after the Tohoku mainshock in box N, a Mj=6.4 earthquake occurred 24 hours after the Tohoku earthquake in box A, and a Mj=6.4 earthquake struck about 4.5 days after the Tohoku earthquake at the base of Mt. Fuji (just west of box R). While it might appear that these remote earthquakes are distinct from aftershocks closer to the rupture plane, Figure 1 suggests that it is more likely that they are simply the largest events to occur within the zone of increased seismicity rate.

[6] Remote earthquake triggering was observed at even greater distances but much lower densities following the 1992 M=7.3 Landers and 2002 M=7.9 Denali, earthquakes [*Hill*, 2008]. Nevertheless, the broad seismic excitation for Tohoku is unprecedented, although for the roughly-equivalent 2004 M=9.1 Sumatra, Indonesia, and 2010 M=8.8 Maule, Chile, earthquakes, no M < 4.7 aftershock could be detected.

[7] Sudden increases of post-Tohoku seismicity are observed in regions B (Akita), J (southern Fukushima – northern Ibaraki),

[1]Disaster Prevention Research Institute, Kyoto University, Kyoto, Japan.
[2]U.S. Geological Survey, Menlo Park, California, USA.
[3]Woods Hole Oceanographic Institution, Woods Hole, Massachusetts, USA.

0094-8276/11/2011GL047834

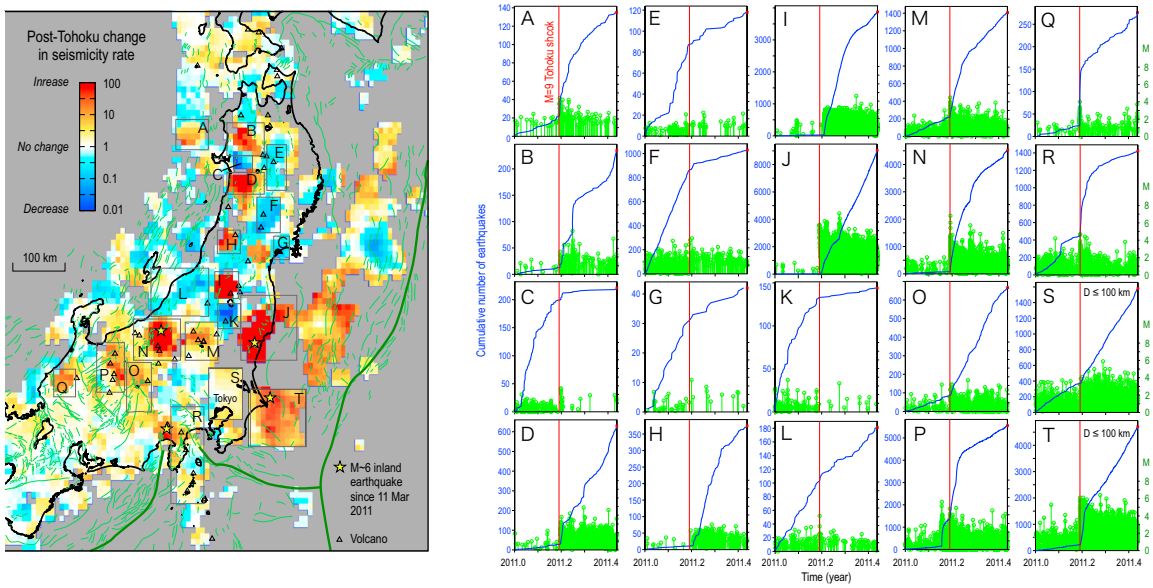

Figure 1. (left) Seismic response of inland Japan to the M=9.0 Tohoku mainshock for Mj ≥ 0.0 seismicity (90 days post-mainshock compared to 1.2-year pre-mainshock), with a smoothing radius of 20 km, using the JMA PDE catalog downloaded on 10 June 2011. Mc is based on *Nanjo et al.* [2010] for inland Japan; Mc could be ~2.0 post-11 March 2011. Except for S and T (0–100 km), all boxes use earthquakes at 0–20 km depth. Dark green lines show plate boundaries. (right) Time series for the boxed regions show cumulative numbers of Mj ≥ 0.0 earthquakes during 1/1–6/10/2011 (blue); each earthquake is shown as a green stem proportional to JMA magnitude, Mj.

T (Cape Inubou), M (Mt. Shirane-Mt. Nantai), S (Kanto), where a burst of seismicity began at the head of Tokyo Bay several days after the Tohoku shock, R (Izu and islands), and P (Hida mountain range) (Figure 1). An increase in seismicity rate apparently delayed by 1–3 days is observed in the box I. The increase in seismicity in regions N and A could be masked by aftershocks of the M ~ 6 mainshocks, or the larger events could be part of the same process. The JMA (Japan Meteorological Agency) PDE catalog normally lists earthquakes that have occurred until two days before present, but because of the enormous number of aftershocks, seismic station damage and power outages, there is some chance that the seismicity rate drops in boxes C, E, F, G, K, and L might be data lapse artifacts. In contrast, the sudden seismicity rate jumps are likely real. Some of the rate increases (boxes A, H, I, M, N, P, Q, and R) exhibit gradual declines since March 11 reminiscent of aftershock sequences, whereas others exhibit a continuous high rate (boxes D, J, O, S, and T).

3. Calculation of the Coulomb Stress Change

[8] The static Coulomb stress change caused by a mainshock has been widely applied to assess areas of subsequent off-fault aftershocks [e.g., *Reasenberg and Simpson*, 1992]. The Coulomb stress change is defined as $\Delta CFF = \Delta\tau + \mu\Delta\sigma$, where τ is the shear stress on the fault (positive in the inferred direction of slip), σ is the normal stress (positive for fault unclamping), and μ is the apparent friction coefficient. Failure is promoted if ΔCFF is positive and inhibited if negative; both increased shear and unclamping of faults are taken to promote failure, with the influence of unclamping controlled by fault friction.

[9] To resolve the Coulomb stress change on a 'receiver fault' (fault receiving stress from a mainshock) requires a source model of the earthquake fault slip, as well as the geometry and slip direction on the receiver. One can assume that the receiver faults share the same strike, dip and rake as the mainshock source fault, one can resolve stress on a major fault of known geometry [e.g., *McCloskey et al.*, 2003], or one can find the receiver faults at every point that maximize the Coulomb stress increase given the earthquake stress change and the tectonic stress [*King et al.*, 1994], termed the 'optimally-oriented' Coulomb stress change. However, the M=9.0 Tohoku earthquake at least temporarily raised the seismicity rate across a region so large that thrust, normal and strike-slip faults co-exist in tectonic stress fields associated with the complex convergence of three tectonic plates. One solution is to resolve the stress change on major active faults [*Toda et al.*, 2011] based on their inferred geometry and slip sense. While this is instructive as a guide to the likelihood that one of these major faults could rupture, the faulting mechanisms of small to moderate shocks that dominate the local seismicity increase are undoubtedly more complex and varied than the associated major structures, and so here we propose an alternative.

4. Use of Focal Mechanisms as Proxies for Small Active Faults

[10] We instead resolve the Coulomb stress changes on the nodal planes of the abundant small earthquakes as proxies for active faults. If the earthquake-induced stress field fundamentally changes the kinds of quakes that can be triggered, this method will fail, as it does at the site of the M=6.6 Iwaki tensional earthquake that produced 30 km of surface normal faulting in a region that was formerly dominated by thrust events. But we will show that most pre-Tohoku mechanisms are consistent with stress transfer to the

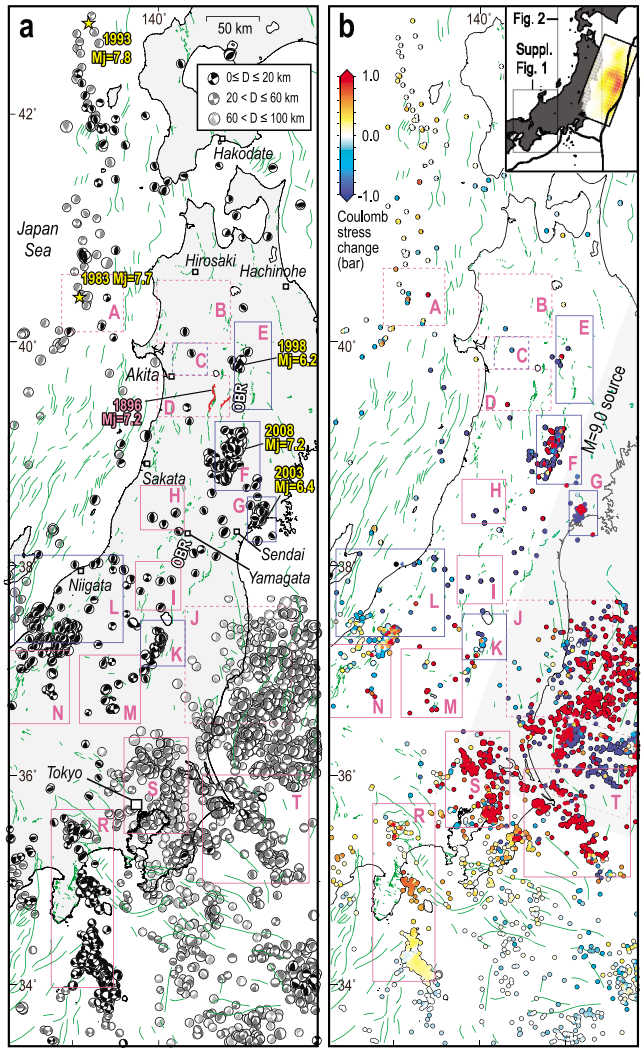

Figure 2. Coulomb stress changes resolved on the nodal planes of small earthquakes as proxies for small active faults. (a) Focal mechanisms from the F-net catalog (http://www.fnet.bosai.go.jp/top.php?LANG=en) since 1997 (depth ≤20 km for inland areas, ≤50 km for the eastern margin of Japan Sea region, and ≤100 km for Kanto); D is depth. (b) Maximum Coulomb stress change from each pair of nodal planes; where earthquakes overlap, the most positively-stressed shocks are plotted on top. The color of the box boundaries indicates the overall seismicity change inside each box: Increase (red) and decrease (blue). Dashed boxes show regions that are not shown in Table 1 for reasons discussed in the text.

aftershocks, and that further, the diversity of the pre-Tohoku mechanisms is much greater than that associated with the major surface faults, and so is more representative of the aftershock faulting.

[11] We make use of fault plane solutions of the full, 14-year-long F-net catalog (http://www.fnet.bosai.go.jp/top.php?LANG=en), which for inland Japan principally includes shallow crustal earthquakes of Mj ≥ 3.5; this corresponds to source dimension ≥400 m [*Wells and Coppersmith*, 1994]. Even though mapped faults [*Research Group for Active Faults in Japan*, 1991] often have sinuous and en echelon traces, comparison of the faults (green lines) with the focal mechanisms in Figure 2a and Figure S1a of the auxiliary material, reveals that the mechanisms exhibit even more complexity, such as strike-slip faults amid the mapped thrust faults of Tohoku, or thrust mechanisms with a wide range of strikes at the site of the 2008 Mj=7.2 Iwate-Miyagi Nairiku earthquake (Figure 2a, box F).[1]

[12] *Toda et al.* [2011] tested six representative source models and three friction values (0.0, 0.4, and 0.8) to determine the model producing the greatest gain in aftershock mechanisms that are promoted by the mainshock, relative to the promotion of the background (pre-Tohoku) mechanisms, which serves as a control population. This was the most rigorous test possible of the Coulomb failure hypothesis that could be applied to the 2011 Tohoku aftershock sequence less than one month after the mainshock. The Wei et al. source model (http://tectonics.caltech.edu/slip_history/2011_taiheiyo-oki/index.html) and a friction of 0.4 produced the greatest (62%) gain, which we use here to calculate the stress changes in an elastic half space with Poisson's ratio 0.25 and shear's modulus 3.2×10^5 bar, using Coulomb 3.3 (www.coulombstress.org). We resolve the static Coulomb stress change on both nodal planes at each hypocenter because we do not know which of the two nodal planes slipped. In Figures 2b, S1b, and S3b of the auxiliary material, we plot the maximum Coulomb stress change for the most positive plane only (we would otherwise have to plot both sets of planes), and also place positive changes (red dots) atop negative changes (blue dots) where earthquakes overlap. Thus, the figures have an intentional 'red bias,' but Table 1 uses both nodal planes and has no bias.

5. Comparison of Seismicity Rate Changes and Coulomb Stress Changes

[13] Comparison of Figure 1 with Figures 2b, S1b, and S3b of the auxiliary material indicates positive associations between observed seismicity rate increases (i.e., aftershocks) and Coulomb stress increases resolved on nodal planes in 11 of the 15 boxes. We find no clear change in stress in one box (Q, Table 1), and negative correlations, which contradict our hypothesis, in 3 boxes (H, I and N). Thus in general, slip on small faults that are revealed by the background focal mechanisms was promoted by the 2011 rupture even when slip on the major faults, as represented by the surface trace and geometry, was inhibited. This means that associated with the major faults are many secondary features, such as ramps, tears, echelons, splays, and antithetical faults, which can be the sites of aftershocks that are triggered by the mainshock rupture even when slip on the major faults is inhibited.

[14] The positive correlations include boxes T and S straddling the rupture, box R located 150–225 km from the rupture surface, and box P, 250 km from the rupture edge. In box S (Kanto district), we included mechanisms as deep as 100 km because of the complex plate configuration beneath Tokyo [*Toda et al.*, 2008]. More than 80% of the stress changes for mid to deeper shocks along the NS-trending 'Kanto seismic corridor' (box S) are positive (Figure 2b).

[1] Auxiliary materials are available in the HTML. doi:10.1029/2011GL047834.

Table 1. The Percentage of Nodal Planes That Experienced a Calculated Coulomb Stress Increase and Average Coulomb Stress Change Compared With the Observed Seismicity Rate Change[a]

Box From Figure 1[b]	Minimum Longitude (deg)	Maximum Longitude (deg)	Minimum Latitude (deg)	Maximum Latitude (deg)	Positive ΔCFF[c] (%)	Average ΔCFF (bar)	Seismicity Rate Change	Correlation Between Rate Change and ΔCFF
E	140.85	141.27	39.42	40.29	7	−1.8	Decrease	Positive
F	140.64	141.14	38.70	39.30	12	−3.3	Decrease	Positive
G	141.00	141.34	38.24	38.64	10	−7.7	Decrease	Positive
H	139.79	140.29	38.34	38.74	0	−3.2	Increase	Negative
I	139.74	140.25	37.55	38.00	0	−2.3	Increase	Negative
K	139.80	140.30	37.04	37.46	13	−1.3	Decrease	Positive
L	138.37	139.61	37.25	38.06	17	−0.6	Decrease	Positive
M	139.10	139.80	36.50	37.15	59	0.6	Increase	Positive
N	138.00	139.00	36.50	37.20	15	−0.4	Increase	Negative
O	137.85	138.38	35.61	36.46	62	0.2	Increase	Positive
P	137.20	137.80	35.95	36.80	87	0.3	Increase	Positive
Q	136.29	136.76	35.88	36.36	44	0.004	Increase	(Negative)
R	138.80	139.50	34.00	35.70	82	0.11	Increase	Positive
S	139.61	140.33	35.48	36.37	83	1.2	Increase	Positive
T	140.50	141.70	35.00	36.00	75	2.5	Increase	Positive

[a]There are two for each earthquake. Because of the preliminary state of the aftershock catalog, the correlations are approximate.
[b]Boxes with less than 10 focal mechanisms excluded.
[c]ΔCFF = Coulomb stress change; ΔCFF positive ≥ 50% (red): <50% (blue). Ave. ΔCFF value ≥ 0 (red); <0 (blue).

[15] There is also a correlation between the (albeit preliminary) seismicity rate decreases and stress decreases in boxes E, F, G, K, and L. Detecting seismicity rate decreases normally requires not only a high rate of preceding seismicity, but also a long post-mainshock catalog that is not yet available. Box F was the site of the 2008 Mj=7.2 Iwate-Miyagi Nairiku earthquake; although the aftershock frequency would be expected to decay, there is an abrupt drop at the time of the Tohoku mainshock. The rate drops in boxes C, F, and K are very large and abrupt, and so may be real.

[16] Inconsistent with the static stress hypothesis, box I shows a delayed rate increase but no stress increase, and there are seismicity rate increases in box A for which Coulomb stress increases are present but do not dominate. Boxes A–D lack sufficient focal mechanisms for confident assessment. Box N, chosen to be centered on the Mj=6.7 shock, shows a rate increase but a stress decrease. Box J is not analyzed because the post-Tohoku seismicity is associated with shallow normal faulting, whereas the focal data contain only deep reverse mechanisms. The boxes with a paucity of pre-Tohoku focal mechanisms (e.g., A, B, and D), and another in which the aftershock mechanisms bear no resemblance to the pre-Tohoku mechanisms (J) challenge this approach. When we resolve the Coulomb stress changes on the post-Tohoku focal mechanisms, we are able to substantially increase the number of focal mechanisms for box J. When we do so, we find that 93% are brought closer to Coulomb failure (Figure S3 of the auxiliary material).

[17] A majority of the mechanisms along the Ou backbone mountain range (boxes B, C, D, F in Figure 2b) are thought to be north-striking thrust faults, which would lie in the principal stress shadow of the Tohoku mainshock, and thus be brought farther from failure [*Toda et al.*, 2011]. However, the significant percentage of strike-slip mechanisms and thrusts of divergent strikes result in a large number of positive stress changes. This underscores that resolving stress on the major faults idealizes the much more complex stress transfer.

[18] We also show all active volcanoes in Figure 1. There does not seem to be any overall association of seismicity rate increases with volcanic regions. Rate increases in boxes M, N, O, P and Q are at least roughly associated with volcanoes, but so are rate decreases in boxes E, F, and K. Further, boxes O and P are associated with the Itoigawa-Shizuoka Tectonic Line (ISTL), and so it is difficult to be certain whether the major active faults or the active volcanoes are more influential.

6. Discussion and Conclusions

[19] The fundamental observation driving this study is the widespread seismicity rate increase across inland Japan, and extending to the Japan Sea and to the Izu island chain. Remarkably, seismicity turned on at distances of up to 300 km from the lower edge of the Tohoku earthquake rupture surface, and up to 425 km from the high (≥15 m) slip zone. These seismicity rate increases are apparent for $M \geq 2$ earthquakes, about half the boxes include $M \geq 4$ earthquakes and in four cases include M=5–6 earthquakes. Most of these increases immediately follow the Tohoku mainshock, but some were delayed by up to several days. These distant aftershocks could be triggered dynamically, they could be caused by the static stress changes, or both. We note, however, that the seismicity rate changes across Japan are not well correlated with the peak ground acceleration recorded by the NIED K-Net/KiK-net strong motion network (Figure S2 of the auxiliary material). Although the ground surface acceleration is enhanced by sedimentary basins, the observed seismicity rate increases and decreases do not appear to be explained by shaking.

[20] The maximum triggering distance, less than two source dimensions from the mainshock, is consistent with the global absence $M \geq 5$ shocks triggered at greater distances [*Parsons and Velasco*, 2011]. Here we adapted the static hypothesis to the special circumstances of triggering on very small faults that are neither optimally oriented in the regional stress field nor parallel to the major faults. We thus

use the Coulomb stress change resolved on the nodal planes of the smallest earthquakes with focal mechanisms, which limits us to M ≥ 3.5 shocks, a ≥400 m rupture scale that at least overlaps that of the aftershocks.

[21] A tentative examination of the observed seismicity rate changes and calculated Coulomb stress changes has met with promising but certainly incomplete success, since we find 11 positive and 3 negative correlations (Table 1). Five of the positive correlations derive from decreases both in observed seismicity rate and calculated Coulomb stress, but it is perhaps too soon to be confident in the seismicity rate declines. Regardless of the process that promotes the aftershocks, we argue that the microseismicity increases demonstrate that the 'remote' Japan Sea and inland Japan shocks (e.g., Mw=6.3 on 3/12 03:59, Mw=6.2 on 3/12 04:46, Mw=5.8 on 3/15, 22:31) are neither exceptional nor truly isolated events. Instead, they simply represent the largest shocks in a very broad zone of elevated seismicity rate that is evident for M ≥ 2 earthquakes.

[22] We also find sites of profound seismicity rate drops, principally in the stress shadow for thrust faulting in inland Tohoku. All five of these sites exhibit calculated Coulomb stress decreases imparted by the Tohoku mainshock on earthquake focal mechanisms, and so they, too, are consistent with the static stress hypothesis. Nevertheless, seismic data gaps during the 3 months after the Tohoku mainshock could produce rate drop artifacts, and so we maintain some caution in their evaluation. In the months ahead, these rate drops will be reassessed.

[23] One of the surprises of this work is that the effect of the stress shadow expected in Tohoku for north-striking thrust fault appears localized. Instead, many sites within Tohoku exhibit an increased rate of seismicity. Here we find that this behavior is nevertheless consistent with static Coulomb stress transfer, but to smaller faults with geometries different from the major faults, a possibility first advanced by *Marsan* [2006]. One important question is whether the activation of these smaller divergent faults could trigger a large event on one of the major thrusts, as might have occurred when the 15 June 1896 M ~ 8-1/4 offshore Sanriku earthquake was succeeded by the 31 August 1896 Mj=7.2 Rikuu inland earthquake at the same latitude (Figure 2a, box D). Since the 2011 Tohoku mainshock is about ten times larger than the Meiji Sanriku mainshock, there could be large changes in intraplate seismicity during the months to years ahead.

[24] **Acknowledgments.** We thank David Hill, Andrea Llenos, and two anonymous referees for thoughtful reviews, and we are grateful to JMA and NIED for the preliminary hypocenter list and focal mechanisms.

[25] The Editor thanks Aaron Velasco and an anonymous reviewer for their assistance in evaluating this paper.

References

Churei, M. (2002), Relationships between eruptions of volcanoes, inland earthquakes (M ≥ 6.2) and great tectonic earthquakes in and around north-eastern Japan Island arc, *J. Geogr.*, *111*, 175–184.

Grunewald, E., and R. S. Stein (2006), A new 1649–1884 catalog of destructive earthquakes near Tokyo and implications for the long-term seismic process, *J. Geophys. Res.*, *111*, B12306, doi:10.1029/2005JB004059.

Headquarters for Earthquake Research Promotion (2005), National Seismic Hazard Maps for Japan (2005), report, 162 pp., Tokyo. (Available at http://www.jishin.go.jp/main/index-e.html.)

Hill, D. P. (2008), Dynamic stresses, Coulomb failure, and remote triggering, *Bull. Seismol. Soc. Am.*, *98*, 66–92, doi:10.1785/0120070049.

King, G. C. P., R. S. Stein, and J. Lin (1994), Static stress changes and the triggering of earthquakes, *Bull. Seismol. Soc. Am.*, *84*, 935–953.

Marsan, D. (2006), Can coseismic stress variability suppress seismicity shadows? Insights from a rate-and-state friction model, *J. Geophys. Res.*. *111*, B06305, doi:10.1029/2005JB004060.

McCloskey, J., S. S. Nalbant, S. Steacy, C. Nostro, O. Scotti, and D. Baumont (2003), Structural constraints on the spatial distribution of aftershocks, *Geophys. Res. Lett.*, *30*(12), 1610, doi:10.1029/2003GL017225.

Nalbant, S. S., S. Steacy, K. Sieh, D. Natawidjaja, and J. McCloskey (2005), Earthquake risk on the Sunda trench, *Nature*, *435*, 756–757, doi:10.1038/nature435756a.

Nanjo, K. Z., T. Ishibe, H. Tsuruoka, D. Schorlemmer, Y. Ishigaki, and N. Hirata (2010), Analysis of the completeness magnitude and seismic network coverage of Japan, *Bull. Seismol. Soc. Am.*, *100*, 3261–3268, doi:10.1785/0120100077.

Nyst, M., T. Nishimura, F. F. Pollitz, and W. Thatcher (2006), The 1923 Kanto earthquake re-evaluated using a newly augmented geodetic data set, *J. Geophys. Res.*, *111*, B11306, doi:10.1029/2005JB003628.

Parsons, T., and A. A. Velasco (2011), Absence of remotely triggered large earthquakes beyond the mainshock region, *Nat. Geosci.*, *4*, 312–316, doi:10.1038/ngeo1110.

Pollitz, F. F., P. Banerjee, R. Burgmann, M. Hashimoto, and N. Choosakul (2006), Stress changes along the Sunda trench following the 26 December 2004 Sumatra-Andaman and 28 March 2005 Nias earthquakes, *Geophys. Res. Lett.*, *33*, L06309, doi:10.1029/2005GL024558.

Reasenberg, P. A., and R. W. Simpson (1992), Response of regional seismicity to the static stress change produced by the Loma Prieta earthquake, *Science*, *255*, 1687–1690, doi:10.1126/science.255.5052.1687.

Research Group for Active Faults in Japan (1991), *Sheet Maps and Inventories*, rev. ed., 437 pp., Univ. Tokyo Press, Tokyo.

Seno, T. (1979), Intraplate seismicity in Tohoku and Hokkaido and large interplate earthquakes: A possibility of a large interplate earthquake off the southern Sanriku coast, northern Japan, *J. Phys. Earth*, *27*, 21–51, doi:10.4294/jpe1952.27.21.

Shimazaki, K. (1978), Correlation between intraplate seismicity and interpolate earthquakes in Tohoku, northeast Japan, *Bull. Seismol. Soc. Am.*, *68*, 181–192.

Toda, S., R. S. Stein, S. H. Kirby, and S. B. Bozkurt (2008), A slab fragment wedged under Tokyo and its tectonic and seismic implications, *Nat. Geosci.*, *1*, 771–776, doi:10.1038.ngeo318.

Toda, S., J. Lin, and R. S. Stein (2011), Using the 2011 M=9.0 Tohoku earthquake to test the Coulomb stress triggering hypothesis and to calculate faults brought closer to failure, *Earth Planets Space*, doi:10.5047/eps.2011.05.010, in press.

Wells, D. L., and K. J. Coppersmith (1994), New empirical relationships among magnitude, rupture length, rupture width, rupture area, and surface displacement, *Bull. Seismol. Soc. Am.*, *84*, 974–1002.

J. Lin, Woods Hole Oceanographic Institution, 266 Woods Hole Rd., Woods Hole, MA 02543, USA.

R. S. Stein, U.S. Geological Survey, 345 Middlefield Rd., Menlo Park, CA 94025, USA.

S. Toda, Disaster Prevention Research Institute, Kyoto University, Gokasho Uji, Kyoto 611-0011, Japan.

GEOPHYSICAL RESEARCH LETTERS, VOL. 38, L00G03, 5 PP., 2011
doi:10.1029/2011GL047834

Auxiliary Material

Auxiliary material for this article contains three figures.

Auxiliary material files may require downloading to a local drive depending on platform, browser, configuration, and size. To open auxiliary materials in a browser, click on the label. To download, Right-click and select “Save Target As…” (PC) or CTRL-click and select “Download Link to Disk” (Mac).

Additional file information is provided in the readme.txt.

Figure S1
Size: 2.8 MB
Format: EPS
Caption: Coulomb stress changes resolved on the nodal planes of the background earthquakes as proxies of local or regional fault structure in Chubu and Kinki districts.

Figure S2
Size: 5.9 MB
Format: EPS
Caption: Seismic response of the entire Japan to the M=9.0 Tohoku mainshock and peak ground acceleration.

Figure S3
Size: 1.8 MB
Format: EPS
Caption: Coulomb stress change on the nodal planes of post-Tohoku earthquakes.

Citation: Toda, S., R. S. Stein, and J. Lin (2011), Widespread seismicity excitation throughout central Japan following the 2011 M=9.0 Tohoku earthquake and its interpretation by Coulomb stress transfer, *Geophys. Res. Lett.*, *38*, L00G03, doi:10.1029/2011GL047834.

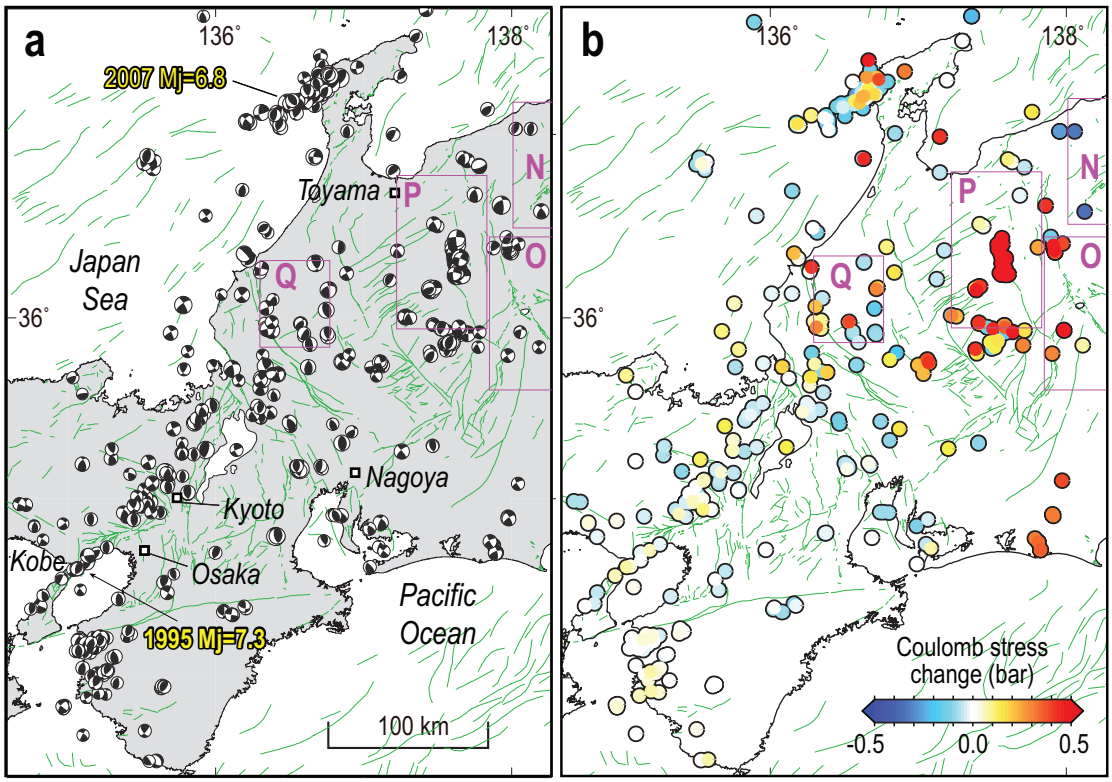

Supplementary Fig. 1

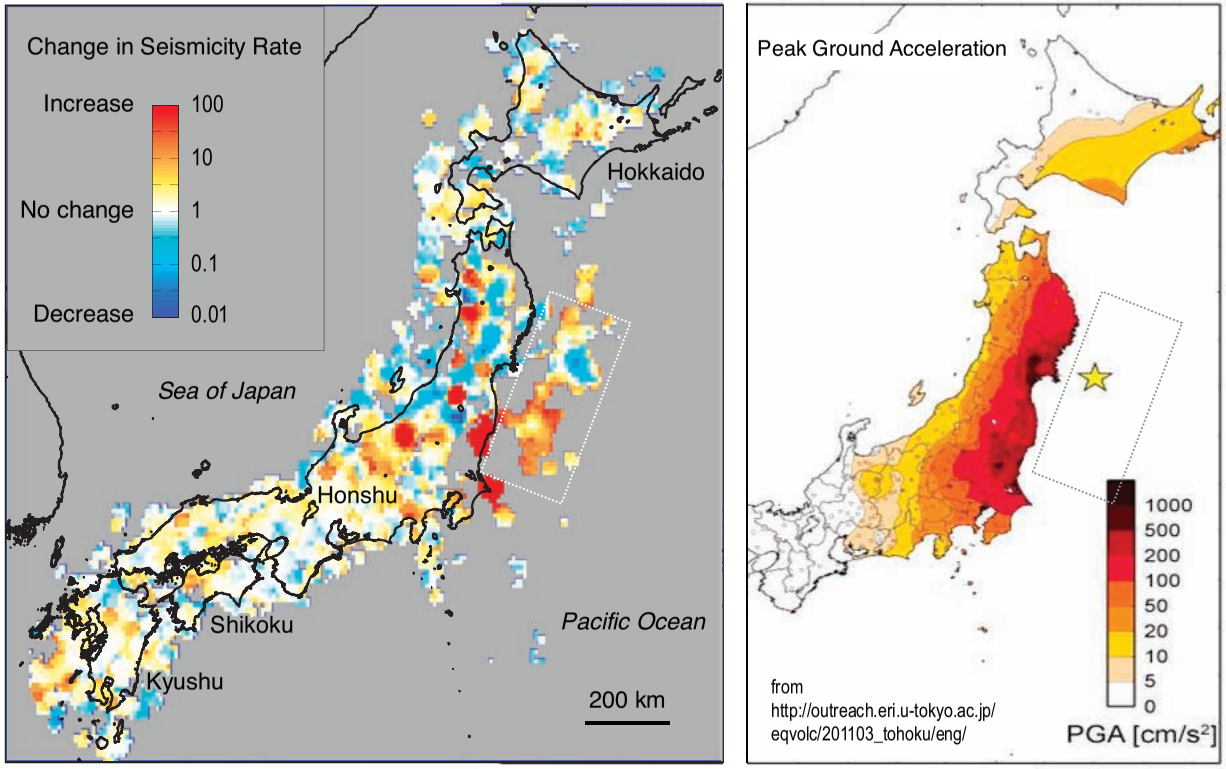

Supplementary Fig. 2

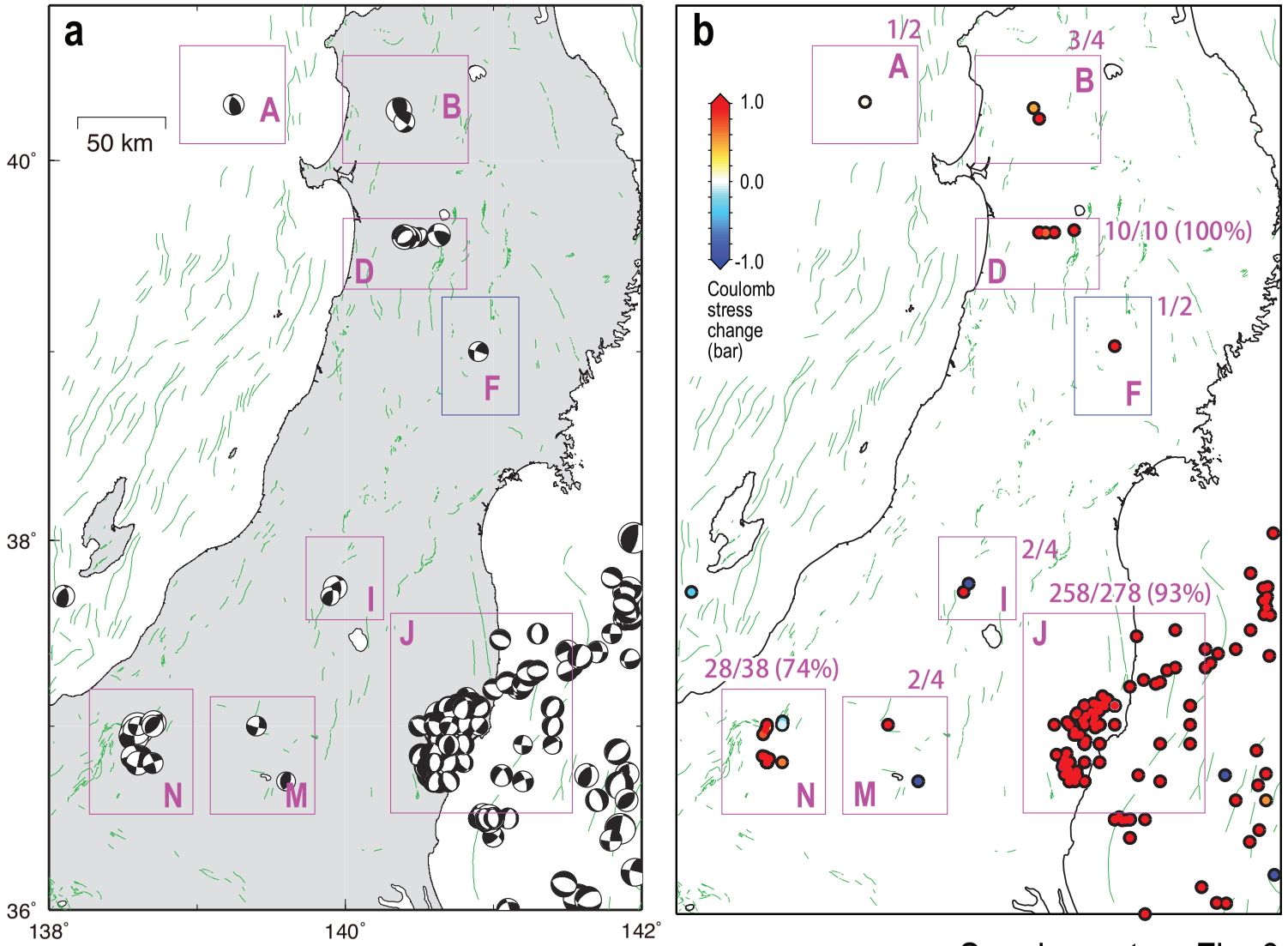

Supplementary Fig. 3